Editors' Suggestion Featured in Physics

Reconstruction of the Instantaneous Earth Rotation Vector with Sub-Arcsecond Resolution Using a Large Scale Ring Laser Array

André Gebauer,[1,2] Monika Tercjak,[3] Karl Ulrich Schreiber,[2,4,5,*] Heiner Igel,[1] Jan Kodet,[2] Urs Hugentobler,[2] Joachim Wassermann,[1] Felix Bernauer,[1] Chin-Jen Lin,[1] Stefanie Donner,[1] Sven Egdorf,[1] Andrea Simonelli,[1] and Jon-Paul R. Wells[4,5]

[1]*Ludwig Maximilians University, Department of Earth and Environmental Sciences, Theresienstrasse 41, 80333 Munich, Germany*
[2]*Technical University of Munich, Research Facility Satellite Geodesy, Arcisstrasse 21, 80333 Munich, Germany*
[3]*Warzaw University of Technology, Department of Geodetic Astronomy, Warsaw 00-661, Poland*
[4]*Dodd Walls Centre for Photonic and Quantum Technologies, Duniden 9054, New Zealand*
[5]*School of Physical and Chemical Sciences, University of Canterbury, PB 4800, Christchurch 8140, New Zealand*

(Received 3 February 2020; accepted 18 June 2020; published 17 July 2020)

Absolute rotation rate sensing with extreme sensitivity requires a combination of several large scale gyroscopes in order to obtain the full vector of rotation. We report on the construction and operation of a four-component, tetrahedral laser gyroscope array as large as a five story building and situated in a near surface, underground laboratory. It is demonstrated that reconstruction of the full Earth rotation vector can be achieved with sub-arcsecond resolution over more than six weeks.

DOI: 10.1103/PhysRevLett.125.033605

Inertial rotation sensors, such as those commonly used for navigational purposes, sense rotation in the presence of bias induced offsets [1]. Very large ring laser gyroscopes [2] operate with vastly reduced bias offsets through the use of state-of-the-art supermirrors with optical losses in the single parts per million range, minimized intracavity optical surfaces, rf excitation of the gain medium, and through their sheer size [3]. These large gyroscopes have been developed to the point that they routinely resolve the rotational velocity of Earth to significantly better than 5 parts in 10^9 [2] with an ability to resolve long period signals such as the Chandler wobble [4,5]. However, single-component gyroscopes will always have an outstanding error source which is uncertainty in the precise position of the optical beams, to the level of accuracy required in applications such as terrestrial tests of the Lense-Thirring frame dragging or other general relativistic precessions [6,7], which demand absolute rotation rate sensing [8,9] with extreme sensitivities.

A solution to this impasse is the development of a large scale, fully three-dimensional sensor which would enable a complete reconstruction of the Earth rotation vector. The gold standard in this regard is the very long baseline interferometry (VLBI) technique [10]. Although accessible in principle, the VLBI measurement technique is not directly linked to the rotational axis of Earth, but to a network of widely spaced radio telescope positions [11]. With the help of modeled nutation and polar motion, the instantaneous orientation of the Earth rotation axis relative to the body of Earth can be inferred. This, however, does not provide the tight local reference required by a large scale single-component gyroscope. Here we describe, and present the initial results of, a solution to this problem through the experimental realization of an integrated multicomponent, large scale optical four-component Sagnac interferometer, called ROMY [12].

ROMY stands for rotational motions in seismology and the system is located at the Geophysical Observatory Fürstenfeldbruck, 20 km west of Munich, Germany, and is constructed as four triangular ring laser structures, arranged in the shape of a tetrahedron, with all corners rigidly tied together. The installation is placed on a massive concrete underground monument with the apex pointing downward. Three of the four triangular gyroscopes have a length of 12 m on each side, while the sides of the horizontal ring on the top is necessarily shorter by 1.0 m in order to fit rigidly on the concrete monument. Figure 1 illustrates the sensor layout at various stages of the construction. The three intracavity supermirrors of each ring completely define the respective scale factor. They are enclosed by tip-tilt adjustable housings mounted on a rigid concrete foundation and connected via stainless steel tubes, thus forming an ultrahigh vacuum recipient, which can be evacuated and filled with a He-Ne gas mixture (0.2 hPa neon and 6.3 hPa helium). Continuous wave laser emission at $\lambda = 632.8$ nm is achieved by rf plasma excitation in a 20 cm long glass capillary with an inner diameter of 5 mm. Apart from the mirror surfaces there are no further optical elements in the cavity. This means that the gain medium fills the entire cavity and the optical losses are minimized.

For laser cavities having perimeters well in excess of 10 m, quality factors much larger than 10^{12} can be achieved, so that the resultant laser linewidth is in the submillihertz regime, and this defines the ultimate sensor resolution. By contrast, a

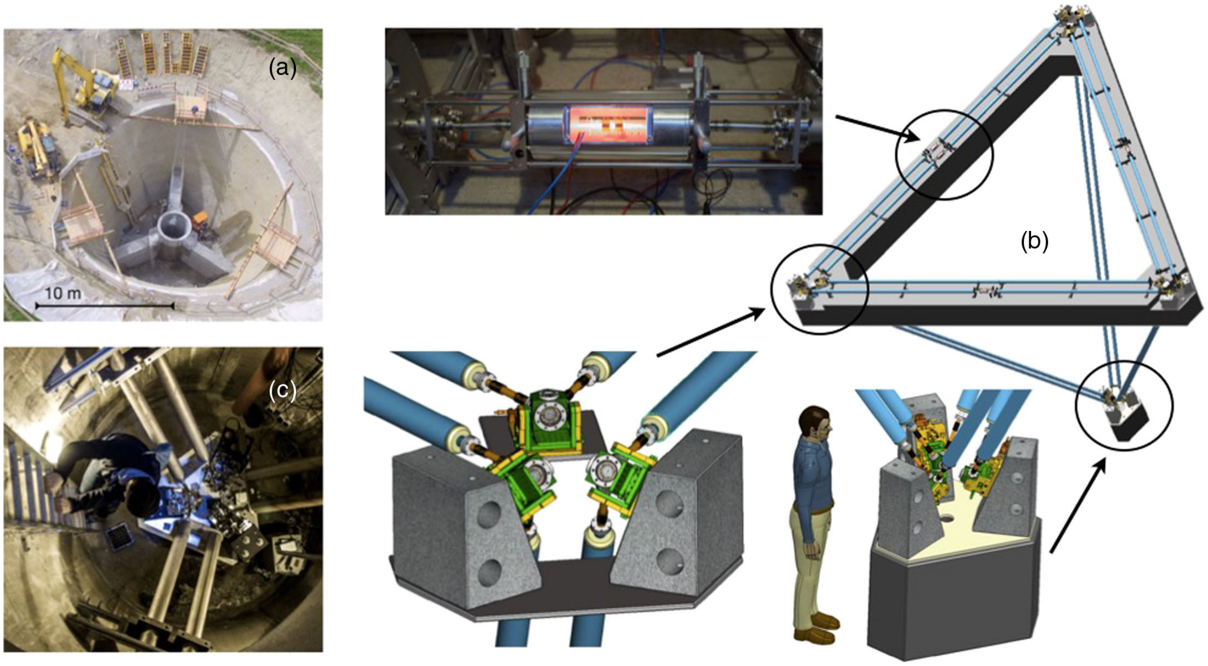

FIG. 1. Construction site of the four-component ring laser structure at the Geophysical Observatory, Fürstenfeldbruck (near Munich, Germany). The excavated location for the monument of the optical resonator (a) provides the room for the tetrahedral gyroscope layout (b). The apex at the bottom of the monument (c) is rigidly attached to the triangular concrete frame on the top by a massive concrete support structure.

passive gyroscope has a cavity resonance several hundred hertz wide. In a bidirectional ring cavity, two counter-propagating laser modes are excited, whose optical frequencies are shifted in opposite directions, when the entire apparatus, rigidly strapped down to Earth, experiences an externally imposed rotation around its area vector. The laser beat note δf of each interferometer component is strictly proportional to the imposed rotation rate Ω_0, with the dimensions of the gyro and the optical wavelength defining the respective scale factor. The beat note is given by $\delta f = 4A/\lambda/P\Omega_0 \cos\phi \cos\theta$, where A is the area enclosed by the laser beams, P the perimeter of the laser cavity, λ the wavelength, ϕ the latitude including the north-south tilt and θ the east-west tilt angle. The latter two quantities describe the orientation of the rotational axis with respect to the plane set up by the laser beams. The measured ringdown times of the cavity exhibiting the best performance produces values of up to 1.130 ms, which delivers a typical sensor resolution of about 10 prad/s obtained after 2 min of averaging for the best ring and 100 prad/s for the worst, as shown from the Allan deviation plot in Fig. 2(a).

The four sensors taken together realize a fully three-dimensional coordinate system, where any combination of three of the four sensors can be used to reconstruct the instantaneous Earth rotation vector relative to the local inertial frame of reference from the beat frequency values. The fourth component offers the possibility to ensure a consistent measurement. Figure 2(a) provides a sketch of the geometry employed. Each side of the tetrahedron represents one ring laser structure, which is sensitive to rotations about the normal vector of the respective plane defined by the laser beams. The whole structure is underground, stabilized by a massive concrete foundation. One of the horizontal corners faces directly south and the beam line on the opposite side runs from east to west. While the length of each side is tightly constrained by the vacuum tubes which enclose the optical cavity, any misalignment of the corners $\delta\alpha$ with respect to the meridian and the tilt angle δz of the entire structure is less well defined. With the horizontal ring given, the orientation of all other rings is constrained, thus forming the full ROMY sensor block. The measured rotation rate of all four rings has been used to establish both the misalignment and the tilt angle δz of the entire ROMY structure with respect to the local horizontal plane. The results for a continuous dataset with a length of 47 days provides a misalignment angle of $\delta\alpha = 0.19205° \pm 0.00042°$. This indicates a very minor rotation of the entire sensor structure toward east. The corresponding tilt angle is $\delta z = -0.07754° \pm 0.00009°$, with the minus sign indicating a tilt toward north.

A geometrically unconstrained resonator is subject to scale factor variations, either directly by slight changes of the geometry of the interferometer or indirectly as a drifting optical frequency causes nonreciprocal frequency shifts through backscatter coupling, or more importantly here, dispersive bias changes. In Fig. 2(c) we show the measured beat note from one of the four rings as an example. Over the ten days for which data are displayed, the ring shows an

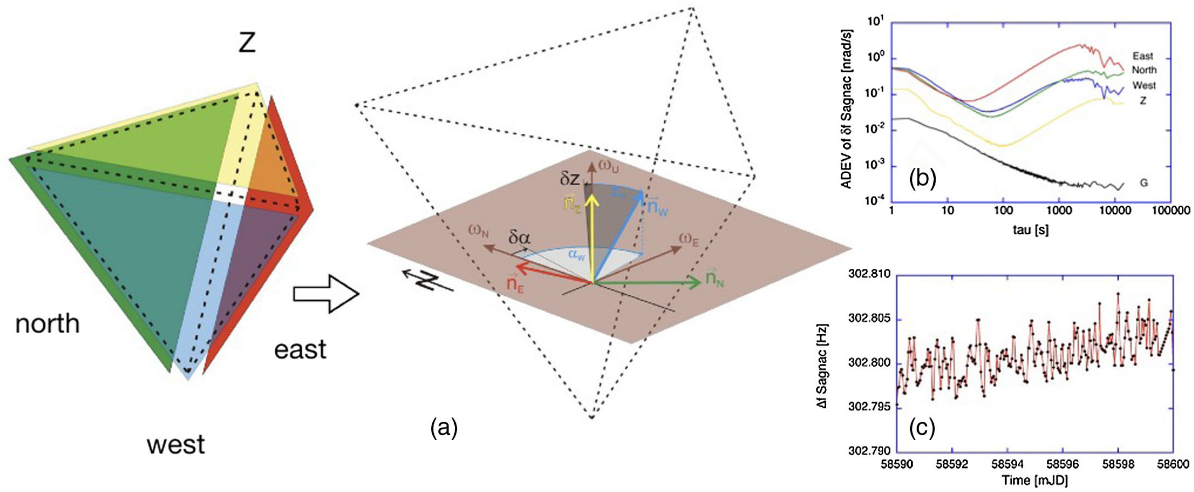

FIG. 2. From the respective normal vectors of all four laser resonators in the tetrahedral structure shown color coded, we can reconstruct the angular rotation in a local north, east, and up ($\omega_{N,E,U}$) system (a). After about 2 min of integration a sensor resolution of 10–100 prad/s is obtained, depending on the respective Q factor of each of the gyros (b). For the best ring this is less than one order of magnitude away from the monolithic G ring laser [2,4], shown in the same graph as a reference (ADEV denotes the Allan Deviation). A sample time series of the Sagnac beat note for the slanted ring on the northern side is shown in (c).

irregular short-term beat note oscillation as the optical frequency drifts and the laser jumps modes as a result of changing temperature. A small overall upward trend is also present as a long-term effect. At this point in time the origin of this small drift is not clearly identified. The most probable cause is a slow drift in orientation of the beam plane, induced by a minute settling of the overall ROMY structure. The observed value would correspond to a slow shift of the beam position of $\approx 160\ \mu$m.

ROMY observes a combination of global Earth rotation and local ground motion. For larger gyroscope installations like ROMY, biases from backscatter coupling are very small. However, larger optical interferometers are more susceptible to mechanical instability than smaller ones [3] and, hence, the dispersive bias shifts. In addition, the free spectral range (FSR) also reduces significantly, with the consequence that the interferometer becomes progressively more sensitive to sudden jumps of the laser mode. For ROMY with a perimeter of $P = 36$ m, the free spectral range ($\mathrm{FSR} = c/P$) is approximately 8.3 MHz. Small variations in the temperature will quickly change the cavity length by more than a wavelength ($\lambda = 632.8$ nm), thus driving the excitation of a different longitudinal mode. By increasing the gas pressure in the ring cavity, the homogeneous linewidth of the gain medium is broadened, which suppresses mode changes for about 100 MHz on either side of the lasing mode [2].

In order to reconstruct the full Earth rotation vector, we have transformed the measured beat note δf_n from each of the four ring laser components [Fig. 2(a)] into a global Earth centered Earth fixed $\omega_{X,Y,Z}$ frame [Fig. 3(a)] and solved the observation equation (1) for the vector $\mathbf{\Omega}_E$.

$$\delta f_n = \kappa_n \mathbf{\Omega}_E \cdot \boldsymbol{n}_n, \qquad \kappa_n = (4 \times A_n)/(\lambda_n \times P_n), \quad (1)$$

with κ_n the respective scale factor of each ring laser component n, $\mathbf{\Omega}_E$ the Earth rotation vector, and A, P, and λ defined as before. The orientation vector $\boldsymbol{n}_n = D \cdot R \cdot \boldsymbol{n}_r$ is composed from the orientation $\boldsymbol{n}_r$ in the local north, east, up ($\omega_{N,E,U}$) frame [Fig. 3(a)], a left-handed system defined by the azimuth angle α_n and the zenith angle z_n [Fig. 2(a)]. The matrix D is used to transform the local observation into the global frame with the longitude θ and latitude ϕ of the ring laser site. For the true orientation, the misalignment matrix R with the offsets δa and δz is applied.

$$\boldsymbol{n}_n = D \cdot R \cdot \boldsymbol{n}_r, \qquad \boldsymbol{n}_r = \begin{bmatrix} \sin z_n \cos \alpha_n \\ \sin z_n \sin \alpha_n \\ \cos z_n \end{bmatrix}, \qquad (2)$$

with

$$\boldsymbol{D} = \begin{bmatrix} -\sin\varphi\cos\theta & -\sin\theta & \cos\varphi\cos\theta \\ -\sin\varphi\sin\theta & \cos\theta & \cos\varphi\sin\theta \\ \cos\varphi & 0 & \sin\varphi \end{bmatrix},$$

$$\boldsymbol{R} = \begin{bmatrix} 1 & -d\alpha & -dz \\ d\alpha & 1 & 0 \\ dz & 0 & 1 \end{bmatrix}.$$

The ω_Z axis is aligned with the Earth rotation axis whilst the ω_X axis passes through the Earth surface where the Greenwich meridian intersects with the equator. The ω_Y axis is oriented 90° toward east in order to form an orthogonal right-handed system. Figure 3(a) illustrates the orientation of the various frames of reference with

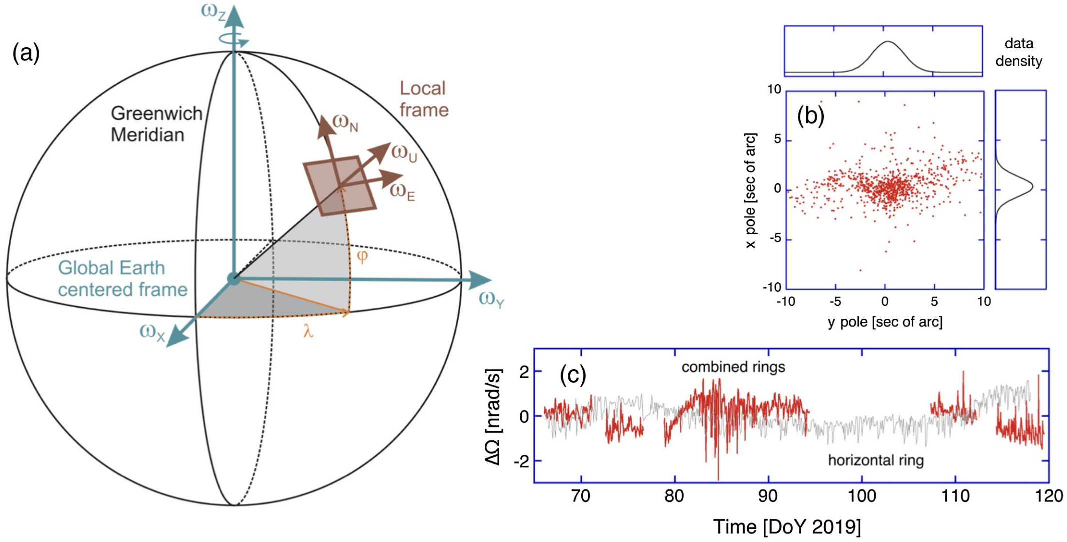

FIG. 3. The angular rotation is measured in the local $\omega_{N,E,U}$ system (a), which subsequently is transformed into a global reference frame. The mean pole position offset (b) is estimated to (0.35 ± 0.022) arcsec in the ω_X direction and (0.47 ± 0.07) arcsec in the ω_Y direction. The instantaneous Earth rotation rate $\Delta\Omega$ is presented with the constant value of the Earth rotation rate $\Omega_0 = 72.921\ \mu\text{rad/s}$ subtracted (c). The gaps in the data occur when the beat frequency values on one or more rings is lost because of laser mode jumps. The results compare well with the residuals of the Earth rotation rate, obtained from the horizontal ring alone when the projection angle is adjusted for a minimum offset (DoY stands for "day of year").

respect to each other. In the global frame of reference, Earth rotation is almost entirely represented in the ω_Z component of the full Earth rotation vector, while ω_X and ω_Y contain the polar motion, a multifrequency signal that is generally small with periods extending from one day to well beyond one year. Figures 3(b) and 3(c) show the initial measurements of the ROMY ring laser structure. Forty-seven days of continuous measurements on at least three sensor components were averaged to hourly values of the instantaneous Earth rotation vector, 1125 in total. We then took the average over all measurements as an estimate of the biased mean pole position, which comes out as (0.35 ± 0.022) arcsec in the ω_X direction and (0.47 ± 0.07) arcsec in the ω_Y direction. The small offset from zero is caused by residual scale factor and bias errors in each ring. The time series of the Earth rotation rate $\Delta\Omega$ is shown in Fig. 3 with a constant value (Earth rate) of $\Omega_0 = 72.921\ \mu\text{rad/s}$ subtracted [Fig. 3(c)]. The reconstructed rotation rate Ω from the combined tilted rings is shown together with the rotation rate residuals obtained from the horizontal ring alone with the projection angle adjusted for a minimum offset. The data gaps occur when one or more rings undergo a mode jump, resulting in loss of the interferogram. In terms of measurement resolution, this time series compares well with the other two components of the Earth rotation vector, indicating that this is the current limitation from the unconstrained cavity.

In summary, we report an internally consistent and highly sensitive, all optical measurement of the full Earth rotation vector utilizing the ROMY four-component large Sagnac gyroscope. Over a length of 47 days, a long-term sensor stability of $\Delta\Omega/\Omega_0$ of 5×10^{-5} and less than 0.5 arcsec for the pole position has been achieved with the four large laser interferometers. After transforming the measurements into the Earth centered Earth fixed frame of reference, a consistent observation of the Earth rotation vector with a repeatability of about 0.1 arcsec was obtained. Small errors in the scale factor and relative orientation of the individual rings with respect to each other are still present, hence the small deviation from zero in the established pole position [see Fig. 3(b)]. The dominant limitation however is the currently unstabilized cavities. The multicomponent assembly overcomes one of the major hurdles to absolute rotation rate sensing with Earth bound laser gyroscopes as outlined by Hurst *et al.* [8], in that for the fully consistent ROMY interferometer the beam planes can be determined with sufficient accuracy of the order of 1 nrad at midlatitudes to make measurements of general relativistic precession feasible in principle. We also note that once all rings are properly drift compensated and with all scale factors fully established, ROMY presents a viable technique for the continuous observation of Earth rotation and polar motion, complementary to the VLBI technique. Eventually the combination of the two measurement techniques together may establish a continuous observation of the Earth rotation vector with high accuracy and temporal resolution.

We gratefully acknowledge support from the European Research Council (ERC-Adv Grant ROMY No. 339991) and additional support from the Ludwig-Maximilians-University Munich. We acknowledge technical support from Mr. Graeme McDonald and Mr. Robert Thirkettle

(University of Canterbury, NZ). (DFG Grant No. GE 3046/1-1 and National Science Centre, Poland, Project No. 2016/23/N/ST10/00355). Figure 1(b) is used by courtesy of FMB GmbH, Berlin, Germany.

*Corresponding author.
ulrich.schreiber@tum.de

[1] R. Rodloff, A laser gyro with optimized resonator geometry, IEEE J. Quantum Electron. **23**, 438 (1987).

[2] K. U. Schreiber and J.-P. R. Wells, Invited review article: Large ring lasers for rotation sensing, Rev. Sci. Instrum. **84**, 041101 (2013).

[3] R. B. Hurst, G. Stedman, K. U. Schreiber, R. J. Thirkettle, R. D. Graham, N. Rabeendran, and J.-P. R. Wells, Experiments with an 834 m^2 ring laser interferometer, J. Appl. Phys. **105**, 113115 (2009).

[4] K. U. Schreiber, T. Klügel, J.-P. R. Wells, R. B. Hurst, and A. Gebauer, How to Detect the Chandler and the Annual Wobble of the Earth with a Large Ring Laser Gyroscope, Phys. Rev. Lett. **107**, 173904 (2011).

[5] W. Tian, On tidal tilt corrections to large ring laser gyroscope observations, Geophys. J. Int. **196**, 189 (2014).

[6] C. W. F. Everitt, D. B. DeBra, B. W. Parkinson, J. P. Turneaure, J. W. Conklin *et al.*, Gravity Probe B: Final Results of a Space Experiment to Test General Relativity, Phys. Rev. Lett. **106**, 221101 (2011).

[7] F. Bosi *et al.*, Measuring gravitomagnetic effects by a multi-ring-laser gyroscope, Phys. Rev. D **84**, 122002 (2011).

[8] R. B. Hurst, M. Mayerbacher, A. Gebauer, K. U. Schreiber, and J.-P. R. Wells, High-accuracy absolute rotation rate measurements with a large ring laser gyro: Establishing the scale factor, Appl. Opt. **56**, 1124 (2017).

[9] A. Tartaglia, A. Di Virgilio, J. Belfi, N. Beverini, and M. L. Ruggiero, Testing general relativity by means of ring lasers. Ring lasers and relativity, Eur. Phys. J. Plus **132**, 73 (2017).

[10] C. Ma, E. F. Arias, T. M. Eubanks, A. L. Fey, A. M. Gontier, and C. S. Jacobs, The international celestial reference frame as realized by very long baseline interferometry, Astron. J. **116**, 516 (1998).

[11] R. Gross, Earth rotation variations–Long period, Treatise Geophys. **3**, 1 (2006).

[12] E. Hand, Lord of the rings, Science **356**, 236 (2017).

[13] See Supplemental Material at http://link.aps.org/supplemental/10.1103/PhysRevLett.125.033605 for the transformations used in this work to go from the local north, east, up frame to the Earth centered Earth fixed frame.